

Remote Single-Molecule Switching: Identification and Nanoengineering of Hot Electron-Induced Tautomerization

Jens Kügel,^{*,†} Markus Leisegang,[†] Markus Böhme,[†] Andreas Krönlein,[†] Aimee Sixta,^{†,‡} and Matthias Bode^{†,§}

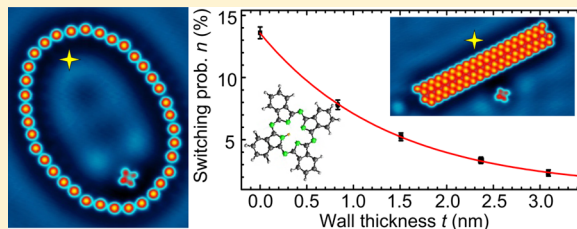
[†]Physikalisches Institut, Experimentelle Physik II, Universität Würzburg, Am Hubland, 97074 Würzburg, Germany

[‡]University of Texas at Austin, Austin, Texas 78712, United States

[§]Wilhelm Conrad Röntgen-Center for Complex Material Systems (RCCM), Universität Würzburg, Am Hubland, D-97074 Würzburg, Germany

S Supporting Information

ABSTRACT: Molecular electronics where single molecules perform basic functionalities of digital circuits is a fascinating concept that one day may augment or even replace nowadays semiconductor technologies. The tautomerization of molecules, that is, the bistable functional position of hydrogen protons within an organic frame, has recently been intensively discussed as a potential avenue toward nanoscale switches. It has been shown that tautomerization can be triggered locally or nonlocally, that is, by a scanning tunneling microscope (STM) tip positioned directly above or in close vicinity to the molecule. Whereas consensus exists that local switching is caused by inelastic electrons that excite vibrational molecular modes, the detailed processes responsible for nonlocal tautomerization switching and, even more important in the context of this work, methods to control, engineer, and potentially utilize this process are largely unknown. Here, we demonstrate for dehydrogenated H₂Pc molecules on Ag(111) how to controllably decrease or increase the probability of nonlocal, hot electron-induced tautomerization by atom-by-atom designed Ag nanostructures. We show that Ag atom walls act as potential barriers that exponentially damp the hot electron current between the injection point and the molecule, reducing the switching probability by up to 83% for a four-atom wide wall. By placing the molecule in one and the STM tip in the other focal point of an elliptical nanostructure, we could coherently focus hot electrons onto the molecule that led to an almost tripled switching probability. Furthermore, single and double slit experiment based on silver atom structures were used to characterize the spatial extension of hot electron packets. The absence of any detectable interference pattern suggests that the coherence length of the hot electrons that trigger tautomerization processes is rather short. Our results demonstrate that the tautomerization switching of single molecules can remotely be controlled by utilizing suitable nanostructures and may pave the way for designing new tautomerization-based switches.



KEYWORDS: Tautomerization, hot electron transport, phthalocyanines, quantum corral, double slit, scanning tunneling microscopy

Since the proposal of single-molecular rectifiers by Aviram and Ratner in 1974,¹ several advanced concepts for molecular electronics have been made (see, e.g., refs 2 and 3 for reviews). In this context the tautomerization of molecules, that is, the interconversion of molecules with the same chemical formula but different structural composition, has often been regarded as a promising concept. For practical realization, the molecule of choice must be immobilized in the gap between two electrodes and at the same time maintain its capability of switching between two tautomers, which may be achieved by protecting the inner region by a robust molecular frame. Ideally, the tautomers shall exhibit different charge transport properties thereby leading to a pronounced on–off ratio in electronic transport.⁴

One critical step toward the realization of tautomerization-based molecular switches is the identification of suitable stimuli that are able to reliably address single molecules and trigger the

transition between tautomers. The scanning tunneling microscope (STM)-induced transition between two tautomers has been shown by Liljeroth and co-workers⁵ where charge carriers are locally injected into naphthalocyanine molecules by positioning an STM tip above. In these experiments, a linear dependence of the switching rate on the tunneling current was found, indicative for a one-electron process. Later experiments on tetraphenyl-porphyrin molecules showed that four-level systems can be achieved by dehydrogenation with only one proton remaining in a 4-fold symmetric molecular cage.⁶

More detailed temperature-dependent and isotope-substituted studies of porphycene molecules performed by Kumagai and co-workers⁷ revealed that tautomerization is triggered by

Received: June 8, 2017

Revised: July 12, 2017

Published: July 21, 2017

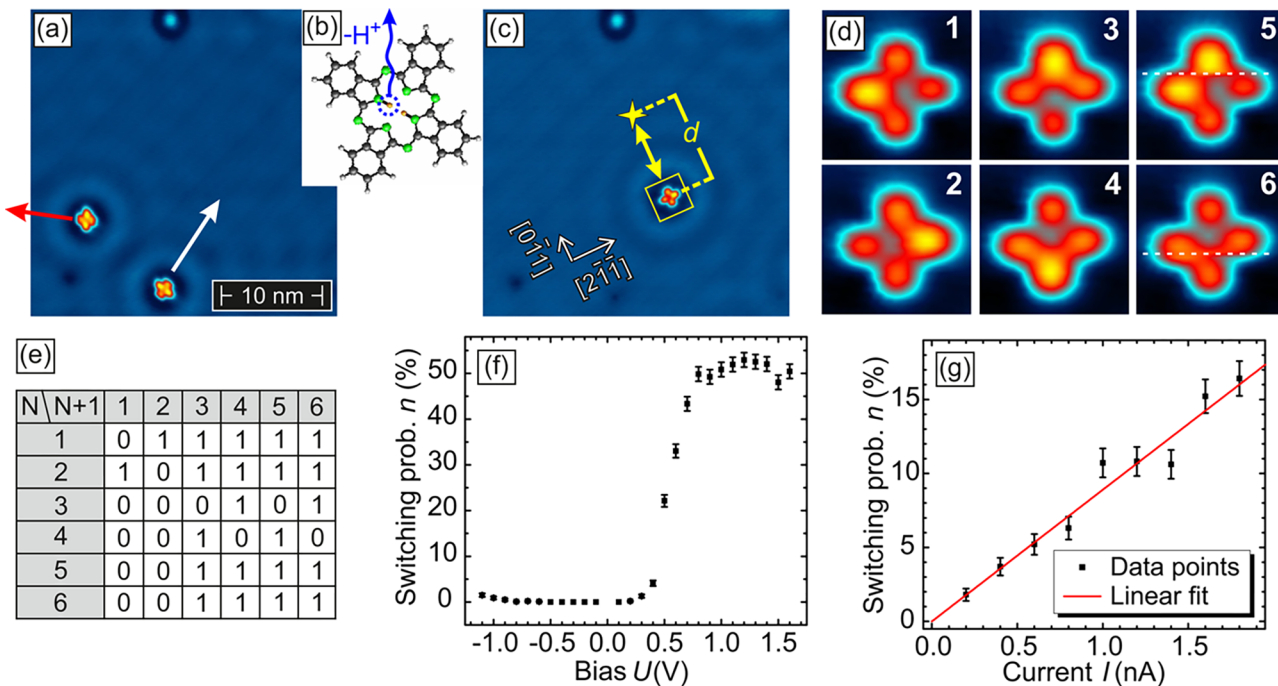


Figure 1. (a) Topography of H₂Pc molecules on Ag(111). (b) Structural model of an H₂Pc molecule consisting of nitrogen (green), carbon (gray), and hydrogen (white and yellow) atoms. Dehydrogenation is indicated by a blue arrow. (c) Same sample location as (a) but after movement, rotation, and dehydrogenation of the molecule. For nonlocal STM-induced molecular excitation, the tip is positioned at the yellow cross where scan parameters are changed for five seconds. Afterward the resulting state is probed by scanning the yellow frame. (d) Six states can be distinguished: Two stable (1 and 2), two metastable (3 and 4), and the same two metastable states (5 and 6) that switch back to a stable state during the scan (see white dashed line). (e) Successive scans ($N \rightarrow N + 1$) are evaluated on the basis of a matrix. Switching event can safely be concluded only where the entry is 1. (f) Bias-dependent switching probability of the nonlocal excitation (excitation parameters: $I = 1$ nA, $d = 2$ nm, 1000 averages). (g) Current-dependent switching probability showing a linear increase (excitation parameters: $U = 0.5$ V, $d = 5$ nm, 1000 switching events).

inelastic process which excite N–H stretching modes with an excitation barrier of 168 meV. Interestingly, single metal adatoms places in close proximity ($\approx 0.5\text{--}2.0$ nm) to the molecule led to a non monotonic distance-dependent variation of the STM-induced tautomerization rate, which on the basis of density functional theory (DFT) calculations, was explained by a modification of the energy barriers that affect hydrogen-transfer rates.⁸ Furthermore, the trans \rightarrow cis tautomerization switching of single porphycene molecules could not only be induced with the molecule placed directly under the STM tip during a voltage pulse but also remotely, *that is, when charge carriers are injected at a distance of a few nanometers from the molecule into the bare Cu(111) substrate*.⁹ The experimentally observed exponential decay with increasing tip–molecule distance-dependent as well as an asymmetric bias voltage dependence indicated a significant contribution of the Cu(111) surface state to a hot carrier-induced process. It shall be noted that in addition to injection by means of an STM tip hot carriers may also be created by light pulses.¹⁰ Next to the triggering of tautomerization, hot carrier excitation have also been shown to drive conformational changes,¹¹ dissociation,¹² or the desorption¹³ of molecules.

In this work, we investigate if and to what extent engineered atomic-scale nanostructures can be utilized for the manipulation of remote STM-induced single molecule tautomerization. We show that walls consisting of Ag atom rows exponentially damp hot electrons if placed between the injection point and the molecule. An ellipse constructed from 36 Ag atoms was used for focusing the charge carriers injected from the STM tip in one focal point onto a molecule positioned in the other focal

point of the ellipse, leading to a 3-fold increase in the tautomerization probability. By controllably moving the molecule around the focal point, we obtain evidence that the excitation process made responsible for STM-induced tautomerization is not only localized in the center of the molecule but extends to its arms. Double-slit experiments performed to discriminate whether the hot electron has to be considered as a quantum-mechanical wave or a wave packet provide no evidence for interference but rather indicate that the electrons have to be considered as localized particles.

Results and Discussion. Remote Tautomerization Switching. For our study, we used the phthalocyanine molecules adsorbed on a Ag(111) surface. A typical topography image is shown in Figure 1a. As schematically shown in Figure 1b, the molecules exhibit a 4-fold symmetric molecular macrocycle in the gas phase with two hydrogen protons bound in the inner cavity of the molecular frame. Upon adsorption on Ag(111), the arms where hydrogen protons are located show up as the bright arms.^{5,14,15} To ensure that the molecule of interest is not adsorbed on a defect, it is controllably moved by the STM tip to a defects-free surface location (indicated by a white arrow). Parameters during manipulation are $U = 20$ mV and $I = 30\text{--}50$ nA. Furthermore, to avoid the scattering of electrons from nearby molecules, they were moved away from the molecule of interest (red arrow).

Once the molecule is safely located on a clean substrate area, one of the two inner hydrogen protons is removed. This so-called dehydrogenation (or deprotonation) is achieved by a bias voltage of 2.0–2.2 V with the tip positioned over the center of the molecule and results in a reduced threshold bias for

tautomerization,¹⁵ an important prerequisite for some of the experiments shown later. Figure 1c shows the same area after these preparatory procedures, that is, movement, rotation, and dehydrogenation of the molecule. The remaining proton can be switched between four positions by the application of a bias pulse on top of the molecule [cf. Figure 1d left and middle column].¹⁵ Because of the symmetry mismatch between substrate lattice and molecular frame, the degeneracy of the four states is lifted, resulting in two stable states (labeled 1 and 2 in Figure 1d) and two metastable states (3, 4) with a lifetime of a few seconds.¹⁵

Whereas consensus has been achieved that direct STM-induced tautomerization is triggered by the injection of electrons or holes in the molecular frame,^{7,16,17} to the best of our knowledge indirect STM-induced tautomerization has only been investigated in a single report by Ladenthin et al.⁹ In this study, which was performed on porphycene molecules adsorbed on Cu(111), bias voltage and coverage-dependent data evidenced a significant contribution of the Cu(111) surface state to a hot charge carrier-induced process. It remained unclear, however, to what extent these charge carriers, that is, electrons or holes, can be manipulated by appropriate atom-by-atom-assembled nanostructures, whether and up to what level the STM-induced tautomerization processes can be made more efficient, and if diffraction can be used as a design principle toward this goal.

In our experiments, we use a sophisticated measurement scheme to analyze the nonlocal excitation of tautomerization processes of single dehydrogenated H₂Pc molecule, which is schematically shown in yellow in Figure 1c. First, the tip is moved a certain distance d away from the center of the molecule in the substrate's [1̄10] direction, that is, along the metastable arms of the molecule. In a second step, the bias voltage and tunneling current are changed to excitation parameters for 5 s. Afterward, the tunneling parameters are reset to noninvasive parameters ($U = -50$ mV, $I = 100$ pA) and the molecule is quickly (6.6 s) scanned in the downward direction. This procedure is repeated between 1000 up to 8000 times for statistical purpose. For data analysis each topographic image is assigned to one out of six possible tautomerization states, which are shown in Figure 1d. In addition to the before-mentioned two stable (1 and 2) and two metastable states (3 and 4), we distinguished two cases where the metastable state decayed during the scanning process (5 and 6). The scan line at which this switching occurs is marked by a white dashed line in the right column of Figure 1d.

After sorting all topographic images into bins (categories) 1–6, the switching probability between successive scans ($N \rightarrow N + 1$) is extracted based on the matrix shown in Figure 1e. The matrix entries represent whether (1) a switching event can safely be concluded or (0) when the molecule remained unchanged or a switching could not safely be assigned to an STM-induced process. For example, the metastable states (3 and 4) spontaneously decay. Therefore, we did not count the transitions $3 \rightarrow 1;2$ or $4 \rightarrow 1;2$ as STM-induced switching events. Only if the hydrogen proton switches to the other metastable arm, that is, if we observe $3 \rightarrow 4$ or $4 \rightarrow 3$, a tunneling current-induced switching event has occurred. Furthermore, it is not counted as a switching event if the state is not changing, even though multiple switching events could have occurred. Only for states 5 and 6, which show the decay of the metastable state, the observation of the same state in two successive scans is considered as a switching event. In

this case the system has to be repeatedly excited to the metastable state, in order to show another decay of the metastable state. A detailed explanation for all entries of the switching matrix can be found in the Supporting Information. Finally, the switching probability is derived by dividing the sum of all switching events by the number of repetitions we have performed the measurement scheme for, minus one.

The bias dependence of the nonlocal STM-induced tautomerization determined by these measurement and analysis procedures is shown in Figure 1f. Each data point consists of 1000 measurements with an excitation current of $I = 1$ nA obtained at a distance $d = 2$ nm from the center of the molecule. Obviously, the switching probability is strongly asymmetric with respect to the bias voltage polarity. At positive bias voltage, a saturation effect is observed above $U \geq 0.8$ V, whereas the switching probability increases only slightly at negative bias voltage below $U < -0.5$ V. This asymmetry could either be interpreted in terms of a field effect,¹⁸ where the direction of the field is more important for the switching than its absolute value due to permanent dipole moments or by a hot-electron process.^{9,12}

The latter appears to be particularly efficient if electrons or holes are injected into a surface state,¹⁹ such as the Shockley-like state hosted by many face-centered cubic (fcc) (111) metal surfaces.²⁰ In the case of Ag(111), the surface used in our study, the band onset of the electron-like surface state is found at $E \approx -63$ meV,²⁰ such that electron injection at positive bias can proceed via the surface state, whereas holes can only be injected into the bulk bands because no surface state exists for energies lower than -65 meV. In contrast to surface states bulk electronic states are not confined to the surface and, therefore, hot electrons injected into these states have a reduced probability of reaching the molecule. In the case of an electron-induced process, the excitation threshold for positive bias is in good agreement with the local STM-induced excitation, that is, with the tip positioned directly above the molecule, which shows a jumplike increase of the switching rate by an order of magnitude between $U = 0.4$ V and $U = 0.5$ V.¹⁵

To determine the origin of the mechanism responsible for the nonlocal STM-induced tautomerization of H₂Pc on Ag(111), we performed current-dependent measurements. The data presented in Figure 1g were obtained at an excitation bias $U = 0.5$ V and a tip–molecule distance $d = 5$ nm. The switching probability is found to linearly increase with current [see linear fit (red line)], consistent with a hot-electron process. Because the tip height, and therefore the electric field, only changes logarithmically with current,²¹ in the case of a field effect only subtle changes with the current would be expected. In agreement with the interpretation of a hot electron process, we found that occasional tip changes do not significantly change the observed switching probabilities. In the case of an electric field effect, strong deviations would be expected, as the electric field, contrary to the tunneling electrons that can excite the sample system, strongly depends on the tip shape.

Tautomerization through Ag Atom Walls. Once the driving mechanism of the nonlocal excitation is determined, the question arises if and to what extent the tautomerization can be modified by atomically engineered nanostructures. In the context of the sample system used here, H₂Pc on Ag(111), it is particularly tempting to use the Ag substrate as an essentially infinite reservoir for building these nanostructures. Indeed, it has been shown that single silver adatoms can reliably be produced by gently dipping a silver tip into the surface²² (more

details available in [Supporting Information](#)). In a first set of experiments these atoms were used to construct walls between the molecule and the excitation position and to investigate how the tautomerization rate changes as the thickness of the wall is increased. Topographic STM images of the various structures and the dehydrogenated molecule are shown in [Figure 2a–e](#). In each panel, the excitation position is indicated by a yellow cross.

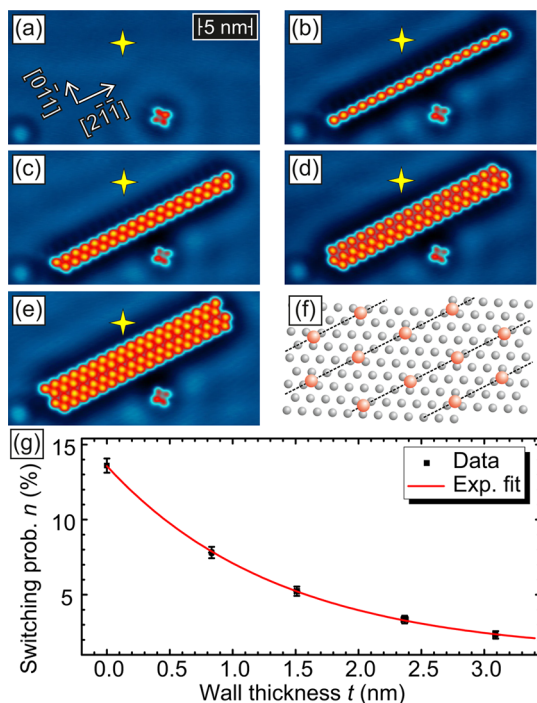


Figure 2. (a) Topography showing the dehydrogenated molecule. The excitation point is marked by a yellow cross. (b–e) Topographic images of the various walls constructed between the molecule and the excitation position by using Ag adatoms and an atom-by-atom assembly process. (f) Atomic model of the walls showing Ag(111) surface atoms (gray) and Ag ad atoms (red). (g) Switching probability n plotted against the fwhm of the wall thickness (excitation parameters: $U = 0.5$ V, $I = 2$ nA, $d = 8$ nm). The data excellently agree with an exponential decay (red).

An atomic model of these walls [cf. [Figure 2f](#)], which was constructed with the help of atomic-scale STM images, reveals that the Ag atoms of different rows are alternately sitting in hexagonal close-packed and fcc sites and the distance between neighboring atoms within a particular row is 1 nm. We investigated the effect of the walls on the nonlocal excitation of the tautomerization by analyzing at least 5000 excitations per data point at excitation parameters $U = 0.5$ V, $d = 8$ nm, and $I = 2$ nA. It should be noted, that we also used at least 5000 excitations for all experiments presented in the remainder. The switching probability n of the pristine sample [[Figure 2a](#)] and each wall [[Figure 2b–e](#)] is plotted against an average full width half-maximum (fwhm) value of the wall thickness in [Figure 2g](#). Obviously, the switching probability decreases with increasing wall thickness t . A single row of Ag atoms reduces the switching probability by roughly 43%. A reduction by up to 83% is obtained for a barrier consisting of four atom rows.

The experimental data can nicely be fitted by an exponential decay law $n(t) = n_b + n_s \exp(-t/\mu)$ [cf. [Figure 2g](#)], with the damping coefficient $\mu = 1.38 \pm 0.32$ nm. This result can be understood in terms of a potential barrier formed by the atom

rows which exponentially damps hot surface state electrons injected from the tip into the sample (n_s). We speculate that the small offset $n_b = (1.05 \pm 0.60)$ % is caused by the contribution of bulk electrons. The good agreement indicates that for the purpose described here the inner structure of the wall's atomic arrangement can completely be neglected. Instead, it appears that, as wall thickness is increased, the average potential height remains constant and a simplified model of potential barriers is fully sufficient to describe the data. It should be noted that the reduction of the switching probability is very unlikely based on the vicinity of the wall atoms to the molecule, as the influence radius of single atoms on the tautomerization, which was analyzed by Kumagai and co-workers,⁸ is roughly four times smaller than the shortest molecule-wall distance s of our measurements ($s \geq 3.5$ nm). Furthermore, the third and fourth atomic row of the wall [cf. [Figure 2d,e](#)] was added on the backside of the wall with respect to the molecule sitting in front of the wall. When adding these rows the electronic properties in the near field of the molecule remain almost unaffected, as can be seen by the standing wave pattern in the topographic images [cf. [Figure 2c–e](#)], whereas the switching probability is strongly reduced.

Focusing of Hot Electrons by an Ellipse. So far we have shown that atomic assemblies can be used to shield a molecule from hot electrons. For potential application, it may be even more relevant if the same principle may also be utilized to enhance the switching probability, for example, by focusing hot electrons onto molecules by means of atomically assembled nanostructures, such as an elliptical quantum corral. This structure, which is well-known from Kondo mirage experiments,^{23,24} is particularly suited because it allows the focus of electrons that were injected into the first focal point to be coherently focused to the second focal point in phase. As shown in [Figure 3a](#) and in the sketch in [Figure 3b](#), we constructed an elliptical quantum corral with a dehydrogenated H₂Pc molecule in one focal point (red molecule).

As shown in [Figure 3c](#) (position 1), the switching probability is almost tripled from $8.65 \pm 0.40\%$ (without ellipse) to $23.54 \pm 0.60\%$ when the molecule is positioned in a focal point of the ellipse. The special geometry of this experiment allows to controllably position the molecule with respect to one focal point, whereas the location where electrons are injected from the STM tip is retained at the other focal point. Thereby, we can examine how sensitive the tautomerization depends on the spatial distribution of hot electrons without bringing the STM tip in close proximity to the molecule, which has been shown to affect the tautomerization.^{5,15} In addition to the settings described above, that is, the bare molecule [black data point in [Figure 3c](#)] and the molecule exactly on the focal point (red), we probed the molecule in three other positions, which are marked by different colors in the sketch [[Figure 3b](#)]. The experimentally determined switching probability is reported in [Figure 3c](#). In comparison to the molecule sitting on the focal point (red), the switching rate is reduced for all three positions. Interestingly, the molecule at the blue position has a lower switching probability than the molecule at the orange position, even though the distance from the center of the molecule to the focal point is smaller in the latter case. This finding may point to the fact that electron-induced tautomerization is more effective if they excite the arm of the molecule rather than the region between the arms. Moving the molecule further away from the focus point (green position) further reduces the switching probability. This experiment demonstrates that the

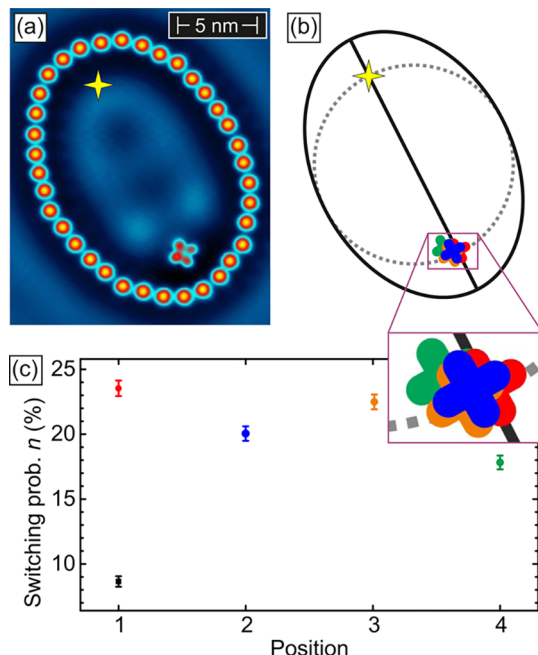


Figure 3. (a) STM image of an ellipse constructed from Ag atoms. A dehydrogenated molecule is located in one focal point, hot electrons are injected from the STM tip positioned in the other focal point (yellow cross). (b) Sketch of the ellipse showing four different measurement positions of the molecule. (c) Molecular switching probability at the positions marked in (b) (same color code applies). The switching rate of the same molecule measured before the construction of the ellipse is shown in black (excitation parameters: $U = 0.5$ V, $I = 2$ nA, $d \approx 12$ nm).

tautomerization rate can be strongly increased by the usage of suitable atomic-scale nanostructures, such as an elliptical quantum corral. The same geometry can also be used as a tool to spatially resolve the tautomerization of molecules sitting close to the second focus point. We would like to mention that the tautomerization state of the molecule also retroactively affects the standing wave pattern of the Ag(111) surface state (not shown here). Even though the effect is very small and therefore hard to detect, it might in future be used for the remote read-out of the molecular configuration.

Double-Slit Experiments. All results presented so far, that is, the current dependency, the exponential reduction of the switching probability by potential barriers, and the strong enhancement of the tautomerization rate by focusing, confirm that a hot electron process is the driving mechanism of nonlocal tautomerization. These experiments provide only very little information, however, on the hot electrons themselves. For example, it remains unclear whether the wave packet of the hot electrons is sufficiently extended to observe diffraction effects. This property can be characterized by a double slit experiment, as localized and delocalized electron wave packet should lead to very different spatial distributions of the switching probability with the molecule being positioned behind the double slit. In the case of very delocalized hot electrons, constructive and destructive interference is expected to result in pronounced maxima and minima of the switching probability behind the double slit. In contrast, very localized electron packets would lead to maxima in the switching probability when the molecule behind the double slit is in the field of view of the injection point.

In order to design a functional double slit from Ag atoms, in a first set of experiments we determined the width-dependent transmission of single slits [Figure 4a,b] by the same kind of tautomerization switching experiments described above. An ideal slit should be sufficiently wide to allow the transmission of the wave packets, while at the same time being as narrow as possible to minimize decoherence of the electron wave packet. As can be seen in Figure 4b, a three-atom-wide slit is a suitable compromise. The transmission through this slit almost leads to the same switching probability as without a wall [cf. red line with dashed error line in Figure 4b]. Reducing the slit width below this value leads to a drastically reduced switching rate due to an unacceptably low transmittability for hot electrons. It should be noted that in the case of a five atom wide slit the switching probability is significantly enhanced, most likely due to the reflection of electrons from the edges of the slit onto the molecule.

To achieve experimentally resolvable maxima and minima, the distance between the two slits should be adjusted to the wavelength of the electron. To reduce the effects of finite molecule size and the discrete grid of possible adatom positions the wavelength should be long as compared to the spatial extension of the objects. As shown in Figure 1f, for H₂Pc on Ag(111) the threshold of STM-induced tautomerization is roughly $U = 0.5$ V. The hot electrons that excite the molecule are mainly injected into the electron-like Ag(111) surface state (onset ≈ -63 meV). By analyzing quasiparticle interference patterns on Ag(111) a wavelength $\lambda = 2.64 \pm 0.14$ nm at the threshold bias value is determined. It should be noted, that the intact H₂Pc molecule would be less suitable for the study presented here because it exhibits a higher tautomerization threshold in comparison to the dehydrogenated molecule.¹⁵ This would lead to a shorter wavelength and, therefore, more tight specifications for building engineered nanostructures.

Taking all these criteria into consideration, we designed a double slit that consists of two three-atom-wide slits, the center of which are separated by a distance of 6 nm. A scaled sketch and the experimental realization of this double slit is shown in Figure 4c,d, respectively. The sketch also schematically includes the two scenarios expected for a wave packet: (i) blue lines represent the wave fronts of the delocalized electron with $\lambda = 2.64$ nm that would result in an interference pattern behind the double slit and the maxima along the directions marked by red lines. In contrast, (ii) for highly localized hot electron wave packets one maximum is expected if the molecule is in the direct field of view [gray triangle in Figure 4c] of the injection point (yellow cross).

We investigated the lateral variation of the switching probability by moving the same molecule relative to the double slit. In total, data from nine molecule positions schematically represented by colored circles in Figure 4c were recorded. The color represents whether the molecule is sitting in a maximum (red), a minimum (yellow), or an intermediate position (orange) of scenario (i), that is, the interference pattern. For four of these nine positions, topographic images are shown in Figure 4d.

Figure 4e presents the experimental result of the measured switching probabilities (black data points). In analogy to Figure 4c, the field of view from the injection point is marked gray. Furthermore, the intensity of the interference pattern as calculated by a simple model, only taking the path differences at the molecule positions into account, is shown as a blue line. Obviously, the experimental data are in disagreement with what

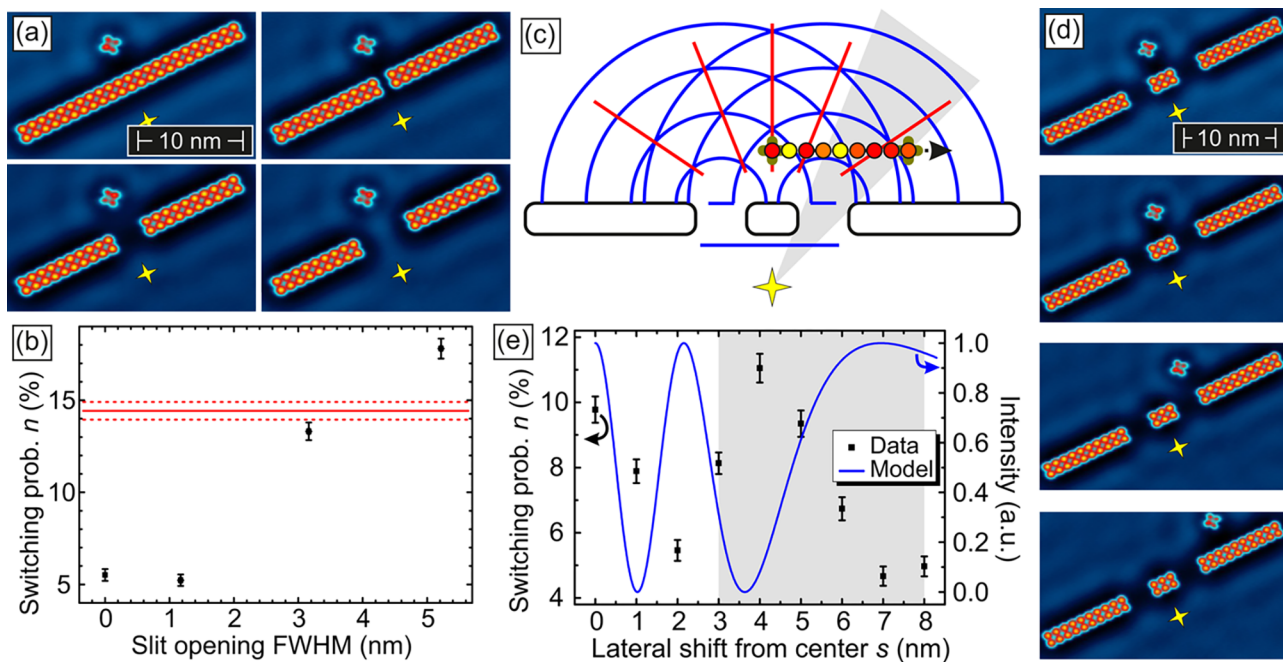


Figure 4. (a) Topographic images of a Ag atom walls with different slit widths. Electrons were injected at the yellow cross. (b) Switching probability plotted against the respective slit width (fwhm) (excitation parameters: $U = 0.5$ V, $I = 2$ nA, $d = 8$ nm). Red line: Switching probability of the molecule without any wall (error bars, dashed lines). (c) Scaled schematic drawing of the double slit showing the excitation point (yellow cross), the field of view from injection point (gray triangle), the waves fronts (blue lines) expected for a wavelength of 2.64 nm with interference maxima (red lines), and the nine experimentally examined positions of the molecule (colored circles). The color of the circle illustrates if the molecule sits in a maximum (red) or a minimum (yellow) of the interference pattern. (d) Topographic images of four of the nine molecular positions behind the double slit. (e) Switching probability of the molecule (black points) in the nine different positions behind the double slit (excitation parameters: $U = 0.5$ V, $I = 2$ nA). The blue line describes the normalized intensity expected within a simplified interference model. The gray area marks the field of view from the tip position.

we expect for interfering electron wave packets. For example, the modeled intensity peaks at a distance $s \approx 2$ nm and $s \approx 7$ nm, where experimentally determined switching rates are particularly low. Beyond that the model predicts a minimum intensity at $s \approx 3.7$ nm, exactly where the highest switching probability is found. It should be noted, that the standing wave pattern formed by the scattering of the surface state electrons is not consistent with the features we observed in the switching probability. This can also be seen in the [Supporting Information](#).

In contrast, the data are in reasonable agreement with our expectations for very localized electron wave packets. With the molecule sitting in the center behind the wall, the switching probability is relatively high for the following reasons: The injection point is positioned axisymmetric to the molecule with respect to the double slit, leading to an enhanced amount of electrons reflected from the edges of the left and right slit to the molecule. Furthermore, the effective thickness of the tunneling barrier is quite small at this position, as an electron packet can tunnel straight through the barrier to reach the molecule. By laterally shifting the molecule about $s = 1\text{--}2$ nm, the effective thickness of the tunneling barrier is enhanced in the case of electrons moving diagonally through the wall. When the molecule partially reaches the field of view of the injection point (distance of $s = 3$ nm), the switching probability sharply increases. The decrease at higher distances ($s \geq 5$ nm) is most likely caused by the enhanced distance between the injection point and the molecule, which inevitably also changes when moving the molecule parallel to the wall. In total, the double slit experiment performed here indicates that the hot electrons that

trigger tautomerization on HPc/Ag(111) can be treated as small wave packet without any detectable self-interference effects.

This result is somewhat unexpected, as the phase coherence length of surface state electrons is usually much longer than the width of the double slit presented in [Figure 4](#). For example, the analysis of interference patterns observed by means of low-temperature STM dI/dU spectroscopy in triangular Ag(111) resonators revealed a coherence length of >30 nm in the energy range up to 0.5 eV.²⁵ We have to keep in mind, however, that the coherence length critically depends on how energy-selective a particular detection mechanism is. In the dI/dU experiments of ref 25, it is essentially determined by the modulation voltage which typically amounts to a few millivolts only. In our case, in contrast hot electrons are “detected” by tautomerization processes of dehydrogenated H₂Pc molecules on Ag(111). The threshold of this process, which is energetically located at about $eU = 500$ meV, is not very sharp but broadened by about ± 100 meV [cf. voltage dependence in [Figure 1f](#)]. Therefore, at the bias voltage $U = +500$ mV chosen in [Figure 4](#) also electrons with a lower energy can trigger tautomerization processes, although with an efficiency that quickly drops with decreasing bias voltage. This energy window broadening leads to a broader k -window, which inevitably leads to a shorter coherence length of the hot electrons. Future experiments that aim at the detection of quantum mechanical interference effects need to utilize hot electrons with a narrower E and k distribution, for example, by making use of a highly energy-selective excitation process with low intrinsic damping.

In summary, we unambiguously identify the hot electron process as the driving mechanism of nonlocal tautomerization of dehydrogenated H₂Pc/Ag(111). We could demonstrate that the tautomerization probability can be tuned over a wide range by making use of engineered silver atom structures. Silver atom walls between the molecule and the injection point act as potential walls, thereby reducing the transmission of the hot electrons by up to 83% for four-atom wide wall. Conversely, the switching probability can be almost tripled by an elliptical arrangement of silver atoms, where the molecule is located in one focal point and electrons are injected in the second focal point. The absence of an interference pattern in a double slit experiment indicates that the coherence length of the hot electrons that trigger tautomerization is relatively short.

Methods. For the STM measurements, a silver tip was used, which was electrochemically edged with a 10% solution of ammonia. H₂Pc (Alfa Aesar) molecules were purified by degassing them under ultrahigh vacuum conditions for more than 2 days. The Ag(111) surface was prepared by cycles of Ar⁺ sputtering at an ion energy of 0.5 keV and subsequent annealing to 700 K. After the final annealing cycle, the sample was cooled to room temperature and the H₂Pc were evaporated at a rate of 0.02 molecular layers per minute. Finally, the sample was brought in our home-built LT-STM, which operates at a temperature of $T \approx 4.5$ K.

■ ASSOCIATED CONTENT

Supporting Information

The Supporting Information is available free of charge on the ACS Publications website at DOI: [10.1021/acs.nanolett.7b02419](https://doi.org/10.1021/acs.nanolett.7b02419).

Explanation for the elements of the switching matrix; silver atom production; adsorption site analysis of the molecule ([PDF](#))

■ AUTHOR INFORMATION

Corresponding Author

*E-mail: jens.kuegel@physik.uni-wuerzburg.de.

Notes

The authors declare no competing financial interest.

■ REFERENCES

- (1) Aviram, A.; Ratner, M. A. *Chem. Phys. Lett.* **1974**, *29*, 277–283.
- (2) Joachim, C.; Gimzewski, J.; Aviram, A. *Nature* **2000**, *408*, 541–548.
- (3) Xiang, D.; Wang, X.; Jia, C.; Lee, T.; Guo, X. *Chem. Rev.* **2016**, *116*, 4318–4440.
- (4) Prasongkit, J.; Grigoriev, A.; Ahuja, R.; Wendin, G. *Phys. Rev. B: Condens. Matter Mater. Phys.* **2011**, *84*, 165437.
- (5) Liljeroth, P.; Repp, J.; Meyer, G. *Science* **2007**, *317*, 1203–1206.
- (6) Auwärter, W.; Seufert, K.; Bischoff, F.; Ecija, D.; Vijayaraghavan, S.; Joshi, S.; Klappenberg, F.; Samudrala, N.; Barth, J. V. *Nat. Nanotechnol.* **2011**, *7*, 41–46.
- (7) Kumagai, T.; Hanke, F.; Gawinkowski, S.; Sharp, J.; Kotsis, K.; Waluk, J.; Persson, M.; Grill, L. *Phys. Rev. Lett.* **2013**, *111*, 246101.
- (8) Kumagai, T.; Hanke, F.; Gawinkowski, S.; Sharp, J.; Kotsis, K.; Waluk, J.; Persson, M.; Grill, L. *Nat. Chem.* **2013**, *6*, 41–46.
- (9) Ladenthin, J. N.; Grill, L.; Gawinkowski, S.; Liu, S.; Waluk, J.; Kumagai, T. *ACS Nano* **2015**, *9*, 7287–7295.
- (10) Böckmann, H.; Liu, S.; Mielke, J.; Gawinkowski, S.; Waluk, J.; Grill, L.; Wolf, M.; Kumagai, T. *Nano Lett.* **2016**, *16*, 1034–1041.
- (11) Schendel, V.; Borca, B.; Pentegov, I.; Michnowicz, T.; Kraft, U.; Klauk, H.; Wahl, P.; Schlückum, U.; Kern, K. *Nano Lett.* **2016**, *16*, 93–97.

- (12) Maksymovych, P.; Dougherty, D. B.; Zhu, X.-Y.; Yates, J. T. *Phys. Rev. Lett.* **2007**, *99*, 016101.
- (13) Sloan, P. A.; Sakulsermsuk, S.; Palmer, R. E. *Phys. Rev. Lett.* **2010**, *105*, 048301.
- (14) Sperl, A.; Kröger, J.; Berndt, R. *Angew. Chem., Int. Ed.* **2011**, *50*, 5294–5297.
- (15) Kügel, J.; Sixta, A.; Böhme, M.; Krönlein, A.; Bode, M. *ACS Nano* **2016**, *10*, 11058–11065.
- (16) Fu, Q.; Yang, J.; Luo, Y. *Appl. Phys. Lett.* **2009**, *95*, 182103.
- (17) Kumagai, T. *Prog. Surf. Sci.* **2015**, *90*, 239–291.
- (18) Alemani, M.; Peters, M. V.; Hecht, S.; Rieder, K.-H.; Moresco, F.; Grill, L. *J. Am. Chem. Soc.* **2006**, *128*, 14446–14447.
- (19) Rusimova, K.; Bannister, N.; Harrison, P.; Lock, D.; Crampin, S.; Palmer, R.; Sloan, P. *Nat. Commun.* **2016**, *7*, 12839.
- (20) Reinert, F.; Nicolay, G.; Schmidt, S.; Ehm, D.; Hüfner, S. *Phys. Rev. B: Condens. Matter Mater. Phys.* **2001**, *63*, 115415.
- (21) Tersoff, J.; Hamann, D. R. *Phys. Rev. B: Condens. Matter Mater. Phys.* **1985**, *31*, 805–813.
- (22) Limot, L.; Kröger, J.; Berndt, R.; Garcia-Lekue, A.; Hofer, W. A. *Phys. Rev. Lett.* **2005**, *94*, 126102.
- (23) Manoharan, H.; Lutz, C.; Eigler, D. *Nature* **2000**, *403*, 512–515.
- (24) Fiete, G. A.; Hersch, J. S.; Heller, E. J.; Manoharan, H. C.; Lutz, C. P.; Eigler, D. M. *Phys. Rev. Lett.* **2001**, *86*, 2392–2395.
- (25) Braun, K.-F.; Rieder, K.-H. *Phys. Rev. Lett.* **2002**, *88*, 096801.